

Atmospheric N₂O Formation via UV-photodissociation of O₃

Brian Schwartz

Physics Department, Swarthmore College

Submitted for the completion of the Honors Program, Spring 1997
Research Performed during summer 1996 at SRI International, Menlo Park, CA,
as a National Science Foundation REU Fellow.

Abstract

Nitrous oxide, N₂O, is a greenhouse gas that plays a role in atmospheric ozone destruction. Known terrestrial N₂O sources do not account for its abundance (300 ppbv) in the atmosphere. We performed matrix isolation experiments to determine if N₂, reacting with electronically excited O₂ (O₂*^(H)), is an atmospheric N₂O source.

A matrix is a thin crystal formed by depositing a gas onto a substrate sufficiently cold to solidify the molecules. We first looked at N₂O doped in matrices of N₂, O₂, and a mixed N₂/O₂ matrix. This data was used to identify photogenerated N₂O in an N₂/O₂ matrix and determine its matrix environment.

N₂O was formed by irradiating undoped mixed N₂/O₂ matrices with UV light capable of exciting O₂ to O₂*^(H). O₂*^(H) reacts with O₂ to make O₃, which can be dissociated into O₂ and O(¹D). Since N₂ + O(¹D) → N₂O, the mere presence of N₂O in the irradiated sample does not prove O₂*^(H) as an N₂O source. As our apparatus allowed for *in situ* matrix isolation spectroscopy, N₂O and O₃ growth curves were generated and evaluated to determine whether N₂ + O₂*^(H) → N₂O + O occurred. Since our data was inclusive, we propose another matrix isolation experiment to determine whether O₂*^(H) is an N₂O source.

I. Introduction

Atmospheric chemists are looking for new sources of N₂O to account for its concentration in the atmosphere. Known terrestrial sources of N₂O, oceans, soils, fossil fuel use, biomass burning, and fertilizer use, do not account for its concentration. N₂O sinks (loss mechanisms) include its photodissociation and photo-oxidation. Average tropospheric concentration of N₂O was 276 ppbv (parts per billion by volume) in the 18th century. After a slight decrease in concentration in the early 19th century, N₂O concentration began to increase by mid-century and reached 293 ppbv by the mid-1960's. The early 1800's decrease is attributed to low temperatures, and the subsequent

increase to human activities including deforestation, cultivation, fertilizer and fossil fuel use, and biomass burning.¹

Atmospheric N₂O

- A greenhouse gas

Visible light from the sun incident on the Earth's surface is reradiated as infrared (IR) light. The earth radiates this light as a black body, Figure 1.2, according to the Planck distribution,

$$I(\lambda, T) = \frac{2\pi c^2 h}{\lambda^5} \frac{1}{e^{hc/\lambda kT} - 1}.$$

Infrared active atmospheric gases such as CO₂, O₃, and H₂O absorb this radiated energy and trap it in the earth's atmosphere. This phenomenon is called the *greenhouse effect*.

Triatomic molecules such as CO₂, N₂O and O₃ are dipoles, and hence absorb IR light because the interaction Hamiltonian is the product molecule's dipole moment and the photon's electric field. An IR photon can excite one of the three *fundamental vibrational modes* of these molecules if its frequency corresponds with a frequency of one of the modes. The "symmetric stretch" mode is symmetric oscillation, at frequency ν_1 , of the two end atoms about the central atom. The "bending" mode is the oscillation, at frequency ν_2 , of angle the central atom makes with the two others. The "asymmetric stretch" mode is asymmetric oscillation, at frequency ν_3 , of the two end atoms about the central atom. In both stretch modes, ν_1 and ν_3 , the angle the central atom makes with the other atoms remains constant. Figure 1.1 shows N₂O's fundamental modes.

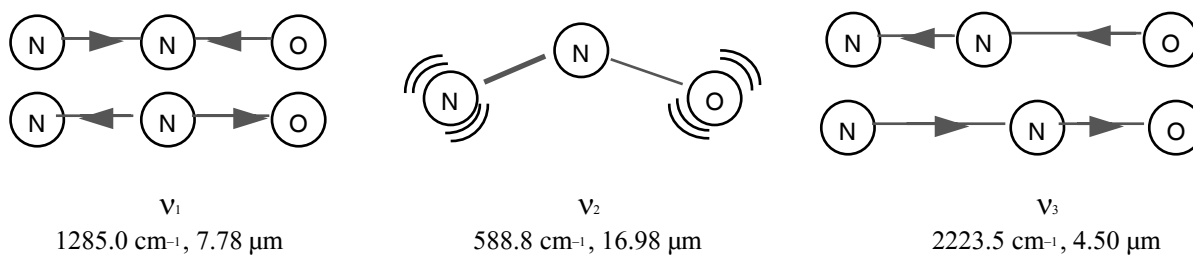


Figure 1.1: Vibrational Modes of the N₂O Molecule and its gas phase vibrational frequencies. The ground state ($\nu=0$) equilibrium N—N bond length is 1.128 Å; N—O bond length is 1.184 Å.²

As shown in Figure 1.2, the Earth does not radiate much at N₂O's strongest IR

absorption band, ν_3 , but the ν_2 and ν_1 modes will absorb radiation that no other greenhouse gases do.

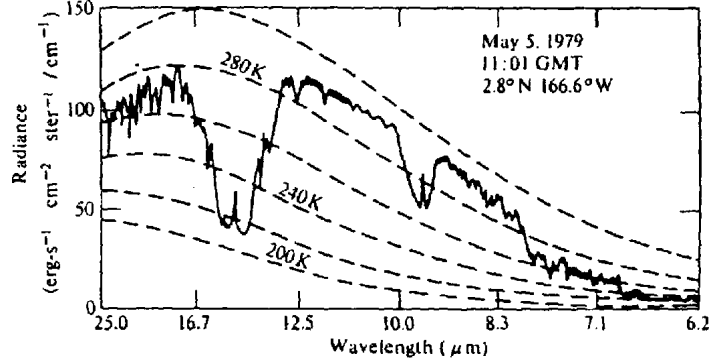
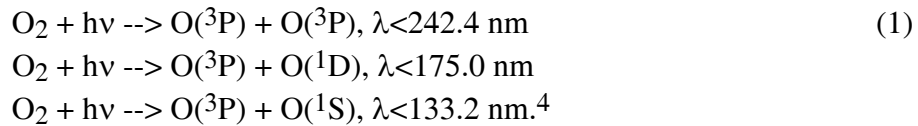


Figure 1.2: The Earth's IR radiation measured in space by a satellite. The higher energy absorbance band is O_3 , and other is CO_2 . Dashed curves are the Planck distribution of black body radiation at various temperatures.³

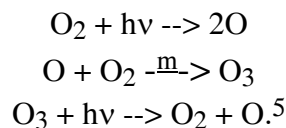
- N_2O and the ozone layer

The troposphere is the region just above the Earth's surface where temperature decreases with altitude. The stratosphere is the region, around 15-50 km above sea level, defined by an increase of temperature with altitude. Ozone in this region plays a large role in this temperature increase, as it absorbs energy from ultraviolet (UV) light in the 210-290 nm wavelength range. Both O_2 and O_3 are formed and dissociated in the stratosphere, which yields a steady state ozone concentration.

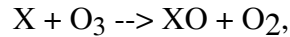
Nitrous oxide is an important atmospheric gas because of its UV absorbance properties and its relation to ozone destruction. Stratospheric O_3 is produced in the *Chapman Cycle*, which begins with the photolysis of O_2 . Relevant O_2 photolysis reactions are:



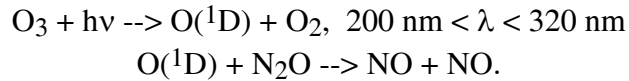
The Chapman cycle begins with O_2 dissociation, which allows O_3 to form and then dissociate to yield an O_2 to begin again the cycle.:



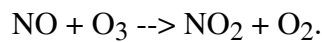
This ozone is also broken down by the catalytic “O_x Cycles”:



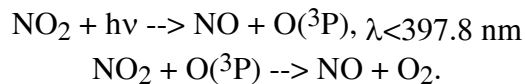
where X can be NO, OH, ClO, BrO. N₂O plays a role in the dominant O_x cycle in the middle stratosphere, the NO_x Cycle:



The nitric oxide (NO) produced in the above reactions consumes ozone:



NO is reformed by NO₂'s photolysis and its reaction with oxygen:



Hence, an N₂O increase in the middle stratosphere increases local NO levels, which makes the NO_x cycle more active in destroying ozone.

In the upper troposphere and lower stratosphere (~7-25 km above sea level), the HO_x cycle dominates the ClO_x and BrO_x cycles, which both are much more active than the NO_x cycle. Increased N₂O concentration increases NO_x activity that produces species such as NO₂, which react with HO_x instead of ozone. Ozone that would have been broken down is left intact because of the increased N₂O. Hence, increased N₂O concentration in the upper stratosphere, unlike an increase in the middle stratosphere, translates into a net ozone increase there.^{5,6}

A New N₂O Source?

Since N₂O plays an important role in the atmosphere, it is valuable to account for its abundance both before and after concentration began to increase in the mid-19th century. Since known N₂O sources cannot account for its abundance in the atmosphere,

discovery of a new source is required to understand and take action regarding increased N_2O levels.

The purpose of this experiment is to discover if N_2O can be formed from the reaction of ground state N_2 with $\text{O}_2^*(\text{H})$, O_2 electronically excited to a ‘‘Herzberg state.’’ The atoms in an oxygen molecule are bound in a 5.13 eV potential well, Figure 1.3. Light with wavelength shorter than $\lambda_{\text{diss.}}=242.4$ nm can dissociate O_2 . States labeled A, A', and c in Figure 1.4 are Herzberg excited states which are electronically excited to less than 1 eV below O_2 's dissociation limit.

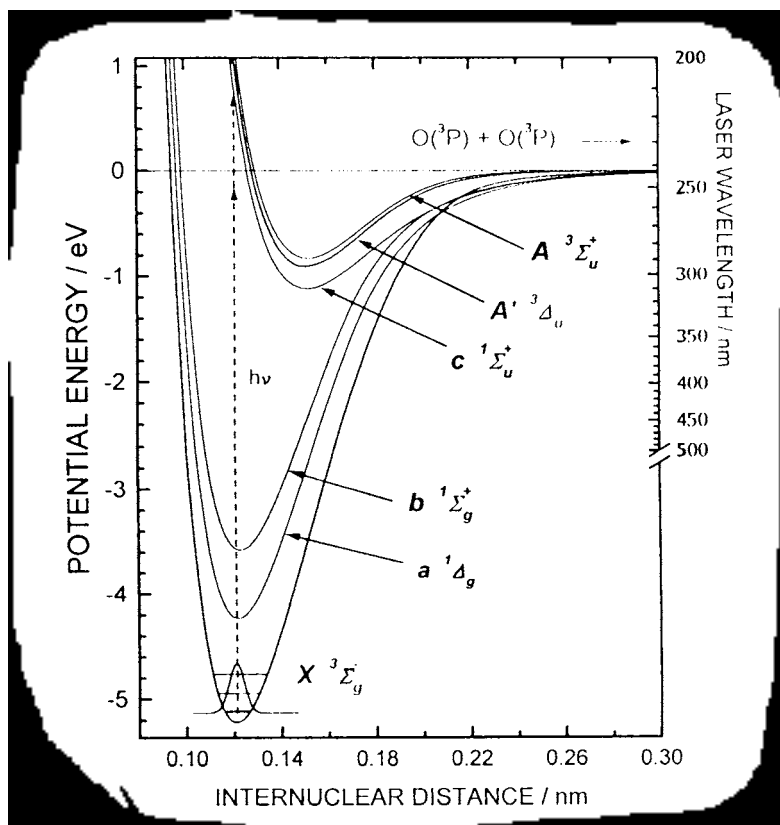


Figure 1.3: Potential curves of the ground state oxygen molecule, O_2 , and electronically excited O_2 states. As shown by the dotted vertical line, absorbance of a $\lambda = 248$ nm photon excites O_2 to one of its Herzberg states $\text{O}_2(\text{A}, \text{A}', \text{c})$, while absorbance of a $\lambda < 242.4$ nm photon dissociates O_2 into two ground state O atoms.^{7,8}

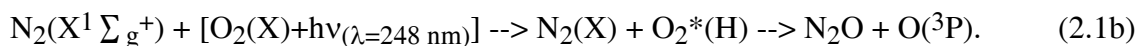
II. Theory

In the gas phase and in an oxygen matrix environment, $\text{O}_2^*(\text{H})$ reacts with ground state O_2 to make $\text{O}_3 + \text{O}$. When O_2 is excited to the 9th vibrational level of $\text{O}_2^*(\text{A})$, the quantum yield of the reaction



is 0.41 ± 0.10 .⁹ While exciting O_2 to higher vibrational levels, $v = 10, 11$, increases the efficiency of (2.1a), 248 nm light, rather than higher energy light, was used in this experiment to excite O_2 because the laser dye capable of lasing in this range had peak power at $\lambda \approx 250$ nm. Since a photon of wavelength 248 nm has energy $hc/\lambda = 5.01$ eV, it excites O_2 to 0.12 eV below its dissociation limit.

Since the atmosphere is 80% nitrogen, an atmospheric $\text{O}_2^*(H)$ is likely to relax to the ground state though *collisional quenching* with N_2 : $\text{O}_2^*(H)$ collides with N_2 and transferring energy to it, leaving O_2 in the ground state. Upon such a collision, N_2 may react with the $\text{O}_2^*(H)$ as the O_2 does in (2), i.e., to form N_2O .¹⁰ While not much is known about this reaction, (2.1b), it is not forbidden by energy considerations. N_2O formation from ground state N_2 and $\text{O}_2^*(H)$ is energetically favorable: more energy is needed to dissociate the reactants into atoms than the products. Ground state N_2 is bound by 9.76 eV while the $\text{N}_2\text{-O}$ in N_2O bond is 1.6 eV.⁴



$$\text{Binding energies (eV):} \quad -9.76 + -0.1 \rightarrow (-9.76 - 1.6)$$

The difference in binding energies of the reactants and products, 1.5 eV, reveals that the O atom in (2.1b) is in its ground state. Had the binding energy difference been greater than the 2 eV difference between the $\text{O}(^3\text{P})$ and $\text{O}(^1\text{D})$ states, the reaction would yield N_2O and $\text{O}(^1\text{D})$. In O_3 , the oxygen atom from the $\text{O}_2^*(H)$ is bound to the O_2 by less than 1 eV.¹¹ Again, the energy difference is less than 2 eV so $\text{O}(^3\text{P})$ is a product of (2.1a).

B. Buijsse et. al. investigated the maximum N_2O production from the reaction of N_2 with $\text{O}_2^*(H)$ in the gas phase.¹² They used 248 nm light to excite the O_2 to the 9th

vibrational level of $O_2(A^3\Sigma_u^+)$. Though the $O_2(X^3\Sigma_g^-)$ to $O_2(A^3\Sigma_u^+)$ transition is forbidden because the states differ in radial symmetries (the - and + in the spectroscopic notation), it occurs because collisional perturbations make excited eigenstates superpositions of unperturbed states involving one with proper symmetry.

The absorption cross section of the $O_2(X) \rightarrow O_2(A^3\Delta_u)$ transition increases from $\sigma = 10^{-24}$ to $\sigma = 10^{-21} \text{ cm}^2$ for oxygen dimers, $(O_2)_2$.¹³ In a matrix, viewed as a collection of O_2 dimers, this forbidden transition is more likely to occur in a matrix environment than a gas environment. Ground state O_2 irradiated with 248 nm light is excited to the 8th or 9th vibrational level of $O_2(A^3\Delta_u)$, depending on its total angular momentum.

Difficulties with Gas Phase Experiments

Ozone can be dissociated by 248 nm light into O_2 and a electronically excited oxygen atom, $O(^1D)$ with 90% efficiency for $\lambda < 300 \text{ nm}$.⁵ Since the reaction,



occurs,^{14, 27} the mere presence of N_2O in a chamber containing both N_2 and $O_2^*(H)$ does not confirm that N_2O is formed from the reaction



Yet, concentration growth curve analysis can reveal the reaction pathway of photogenerated N_2O , i.e., whether it formed via (2.2) alone or by (2.2) and (2.3). Considering (2.2) only, at initial irradiation doses, the slope of the N_2O growth curve is zero because O_3 must be formed and dissociated before N_2O formation can occur. The N_2O growth curve will approach a constant rate after the O_3 concentration reaches a dynamic equilibrium. From this point, O_3 concentration remains constant, and N_2O

concentration will continue to increase with a linear slope, as there are no loss mechanisms for it in the matrix environment. The rate N_2O of concentration will decrease only when there are no other N_2 molecules to bond with $O(^1D)$ formed from O_3 dissociation. These $O(^1D)$ atoms will reform O_3 , as the $O(^1D)$ atoms have no other accessible reaction pathway. Figure 2.1 shows the N_2O and O_3 growth curves.

Since the atmosphere is 80% N_2 , N_2 will not be a limiting reagent in N_2O formation. So where N_2O forms via the bimolecular reaction:

- O_3 concentration grows linearly before reaching a steady state equilibrium concentration.
- N_2O growth rate increases from zero and reaches a constant rate when O_3 concentration is constant in time.

The above process is a *bimolecular reaction*. If O_2 concentration drops and both O_3 and N_2O form via a first order rate law, then

$$\frac{d[O_2]}{dt} = -k_1[O_2] \quad (2.4)$$

$$\frac{d[O_3]}{dt} = k_1[O_2] - k_2[O_3] \text{ and} \quad (2.5)$$

$$\frac{d[N_2O]}{dt} = k_2[O_3].^{14} \quad (2.6)$$

As the intermediary molecule, ozone concentration depends on both its source, O_2 dissociation, and its sink, N_2O formation. In an environment consisting of both N_2 and O_2 , the $O(^1D)$ formed from O_3 dissociation can both reform O_3 and form N_2O ; k_2 is the rate constant of N_2O formation.

Before irradiation, at $t = 0$, the matrix has a concentration of $[O_2]_0$ for oxygen molecules, and zero for O_3 and N_2O . N_2 is an unlimited reagent. Oxygen's rate equation (2.4) can be integrated to yield

$$[O_2] = [O_2]_0 e^{-k_1 t} \quad (2.7)$$

Substituting (2.7) into (2.5) and solving the linear first order differential equation yields $[O_3]$ and $[N_2O]$, plotted in Figure 2.1:

$$\frac{d[O_3]}{dt} = k_1[O_2]_0 e^{-k_1 t} - k_2[O_3]$$

$$[O_3] = \frac{k_1[O_2]_0}{k_2 - k_1} \left(e^{-k_1 t} - e^{-k_2 t} \right) \quad (2.8)$$

$$[N_2O] = \int_0^t k_2[O_3] dt = [O_2]_0 \left[1 - \frac{1}{k_2 - k_1} \left(k_2 e^{-k_1 t} - k_1 e^{-k_2 t} \right) \right] \quad (2.9)$$

The above equations do not take into account that O_3 can be reformed, hence, (8.8) inaccurately has $[O_3]$ decreasing to zero, rather than remaining constant after leveling off. Equation (2.9) is accurate because the N_2O curve should still be “S” shaped, as the growth rate decreases as unbound N_2 concentration decreases. We expect to make little N_2O , so N_2 will be an unlimited reagent, and we do not expect to see the N_2O concentration level off. Figure 2.1 shows only parts of the plots that are accurate for our photogenerated species in the mixed matrix.

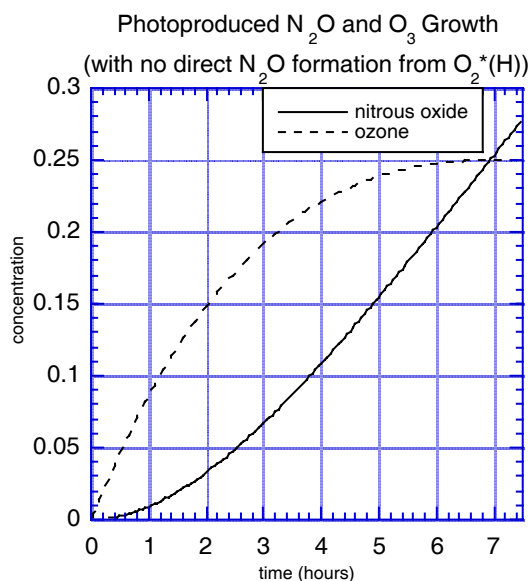


Figure 2.1: Growth curves of N_2O , “S” shaped, and O_3 , linear to 1st order, based on equations (2.8) and (2.9). $[O_2]_0 = 1 \text{ M}$, $k_1 = 0.1 \text{ hr}^{-1}$, and $k_2 = 0.2 \text{ hr}^{-1}$.¹⁴

As shown in Figure 2.1, the initial growth rate of photogenerated N₂O in mixed matrix irradiated to form O₂*(^H) will *nonlinear* because N₂O is formed via the bimolecular process involving O₃ formation and dissociation. The concentration of N₂O formed directly from O₂*(^H) (reaction 2.3) will increase as O₃ does (at initial irradiation doses) in Figure 2.1: *linearly*, because of a constant rate of O₂ excitation to O₂*(^H). Yet, if the direct formation (2.3) occurs, the N₂O growth curve will still be *nonlinear*: the sum of the growth curves of the indirectly formed N₂O and the N₂O formed directly from O₂*(^H).

The nature of the gas phase experiment did not allow *in situ* measurements of N₂O concentration during irradiation, so growth curve analysis was not possible in this set-up. This information is crucial in determining whether O₂*(^H) is an N₂O source because O₃ is also formed from O₂*(^H). Matrix isolation spectroscopy allows for such *in situ* measurements.

Detection of gas phase N₂O made via Herzberg excitation of O₂ was difficult because weak N₂O absorbance bands made even N₂O detection difficult. Matrix isolation spectroscopy eliminates this problem. Unlike N₂O formed in a matrix, N₂O formed in the gas phase can stick to the gas container walls and not be detected. Further, matrix isolated species have little thermal energy and generally have no room to rotate as gas phase molecules do. Matrix absorbance bands are more likely to show the excitation of molecules from vibrational and rotational ground states ($v = j = 0$) to a vibrationally excited $j = 0$ state than those in the gas phase. The dispersion of the gas phase vibrational absorption band is larger than that of matrix isolated N₂O. For low N₂O concentrations this is important, as a narrow strong band is more easily detected above noise than a weak broad one.

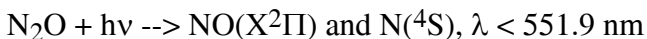
Reactions In a Mixed N₂/O₂ Matrix Irradiated with $\lambda = 248$ nm light

The nitrogen atoms of an N₂ molecule are bound more strongly (-9.76 eV) than the oxygen atoms of an O₂ molecule (-5.1 eV).⁷ Molecular orbital theory explains the

difference. O₂ has two electrons in its 2π* molecular orbital that N₂ lacks. This absence makes N—N bond order 3 while the O—O of O₂ has bond order 2. Bond order is the number of electrons in anti-bonding orbitals subtracted from the number electrons in bonding orbitals. Bonding orbitals have higher probability density between the bonded atoms than anti-binding orbitals, so bond order is a measure of bond strength. High energy UV light (λ < 128 nm) can dissociate N₂. Hence, we will not dissociate any N₂ while exciting O₂ to O₂*(H).

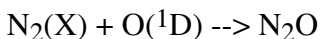
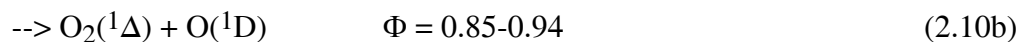
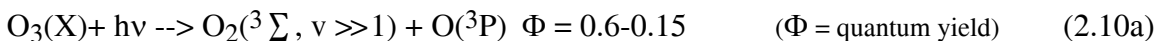
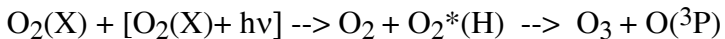
N₂O can be formed by the reaction of N₂(A³Σ_u⁺) and O₂.¹⁷ Since only UV light with in the 180-210 nm range can excite N₂ to N₂(A³Σ_u⁺), we need not consider N₂O formation from this reaction.

The bond energy of the N₂—O bond is 1.672 ± 0.005 eV, and the energy of the N—NO bond is 4.992 ± 0.005 eV. Dissociation reactions are:

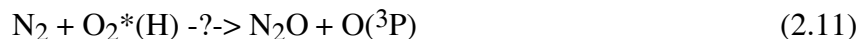


The absorption cross section of N₂O is ~10⁻²⁸ m² at 248 nm while that of O₃ is ~10⁻²³ m².⁴ Since the dissociation of any photogenerated O₃ is five orders of magnitude greater than that of N₂O, we will ignore the dissociation of N₂O by 248 nm light.

The following reactions are known to occur in a mixed matrix irradiated with λ = 248 nm (5.01 eV) light. The quantum yield of (2.10b) plummets from above 0.9 to 0 between 305 nm and 320 nm.^{4,7}



The goal of this experiment is to determine if the following reaction occurs.



Pitts (1986) cites three experimental values for the quantum yield of (2.10b) at 248 nm, 0.85 ± 0.02 , 0.91 ± 0.03 , and 0.94 ± 0.01 .⁵ Quantum yield is an attribute of a reaction, in this case, they are the fraction of dissociated O₃ molecules that form the products in (2.10 a or b). The absorption cross sections, mentioned above, are attributes of the O₃ molecules themselves and their capacity to absorb light of a certain wavelength. Both the absorption cross sections and quantum yields will effect the abundance of photogenerated products formed at different wavelengths.

Matrix Isolation and the Cage Effect

A matrix is a thin crystal formed by depositing a gas onto a substrate sufficiently cold to condense the molecules to a solid. In this experiment, we will be looking at the “guest molecule” N₂O embedded in different “hosts”: an N₂ matrix, an O₂ matrix, and a mixed matrix consisting of half N₂ and half O₂.

The ratio of guest molecules to host molecules, the mixing ratio (MR) will be varied to determine the nature of the matrix isolated N₂O. Since N₂O is a polar molecule (N-N-O),¹⁷ two or more N₂O's in close proximity in the matrix can form complexes. Two N₂O molecules close together and oriented with poles attracting each other form an N₂O “dimer,” (N₂O)₂. Higher order N₂O aggregates are called multimers. Monomer, dimer, and multimer absorptions can be identified by looking at the absorbance of a band as a function of guest species concentration. Dimer and multimer bands will increase as the MR increases.

The frequency at which a matrix isolated molecule vibrational modes oscillate depends on the nature of its host matrix. Shifts from the gas-phase values of a molecules vibrational modes are called *matrix-shifts*. They are caused by interactions between a

guest molecule and the host molecule, collectively known as the “cage effect.” The guest molecule can be seen as trapped in a cage, a unit cell of the host matrix.

Unit cells of α -N₂ and α -O₂ is shown in Figure 2.2. An N₂ matrix at T < 35.6 K is in the α -N₂ phase. Its unit cell volume 181.3 Å³ number density is 22.1 molecules/nm³.¹⁸ An O₂ matrix at T < 23.8 K is in the α -O₂ state. Its unit cell volume 69.44 Å³ number density is 14.4 molecules/nm³.¹⁹ Temperatures 35.6 K for N₂ and 23.8 K for O₂ mark temperatures for matrix phase transitions, above which the matrix structures change to β -N₂ and β -O₂.

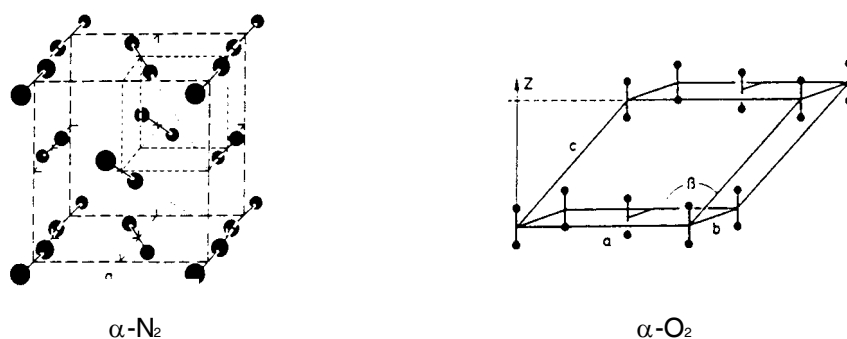


Figure 2.2: Units cells of N₂ and O₂ at 15 K. The face-centered cubic α -N₂ unit cell contains four N₂ molecules, with lattice constant $a = 5.66 \text{ \AA}$. The monoclinic α -O₂ unit cell contains one O₂ molecule, and has dimensions $a = 5.403 \text{ \AA}$, $b = 3.429 \text{ \AA}$, $c = 5.086 \text{ \AA}$.¹⁸

III. Experiment

Apparatus

All experiments were performed at SRI International’s Molecular Physics Laboratory in Menlo Park, California. Matrices were grown on a 10 mm diameter gold coated copper mirror in a steel vacuum chamber. A Fourier Transform Infrared (FT-IR) Spectrometer irradiated was used to detect matrix-isolated species. A “mixing chamber” ($V=2 \times 10^{-5} \text{ m}^3$) was used to store mixed gases to be deposited onto the substrate. The matrix was kept in a vacuum to ensure impurities, e.g., H₂O and CO₂, did not freeze onto the substrate. To minimize IR absorption by impurities, the FT-IR and the light detector were purged with N₂ gas. Figure 3.1 shows the experimental setup.

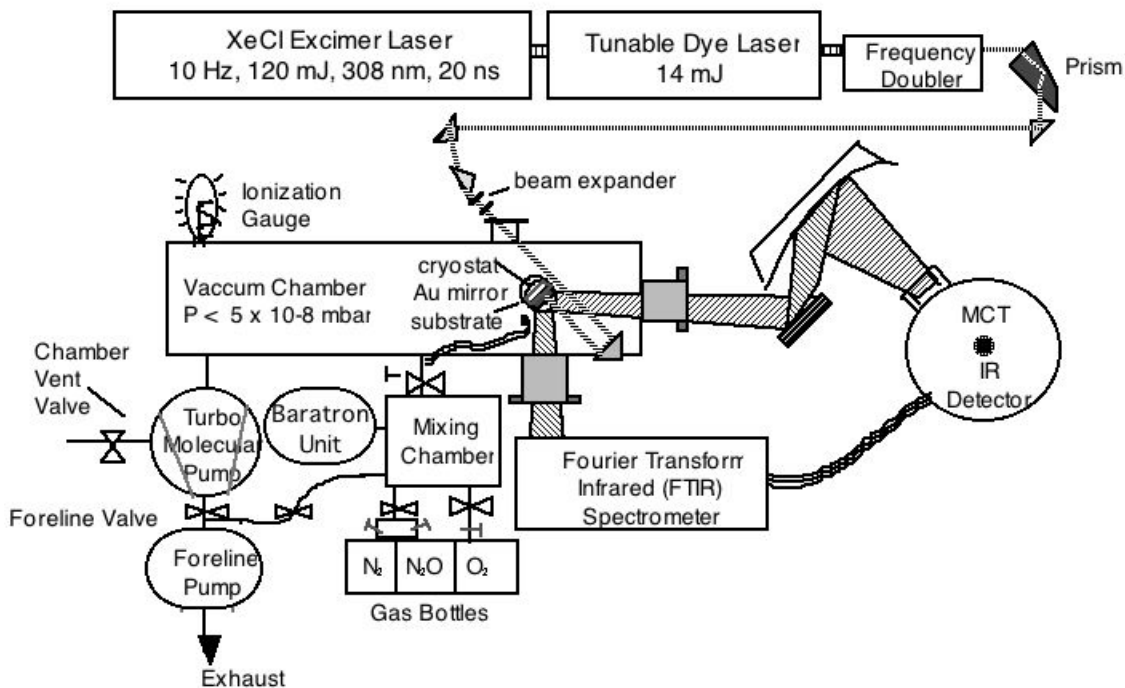


Figure 3.1: Apparatus used for FT-IR Spectroscopy and Laser Irradiation of Matrix Isolated Species

A turbo molecular pump (TMP) and a foreline pump were connected in series between the vacuum chamber and the exhaust. The foreline pump, capable of sustaining a pressure as low as 10^{-3} mbar in the chamber, also served to empty the mixing chamber when necessary. A TMP (Leybold-Heraeus Turbotronik NT 450) kept the vacuum chamber pressure as low as 10^{-8} mbar.

An ionization gauge (Duniway Stockroom Corporation T-100-K) monitored the chamber pressure up to 10^{-4} mbar. The gauge is a bulb enclosing two wires: a heated wire filament surrounding a straight wire under a positive voltage serving as a cathode. The bulb is attached to the vacuum chamber so the gas density of gas in the bulb equals that of the vacuum chamber. Electrons emitted from the filament ionize gas molecules in the bulb, which are attracted to the cathode. Ions collected on the cathode create a current proportional to the pressure in the chamber. A Varian 801tc Vacuum Gauge monitored higher pressures.

A Matheson analog pressure gauge monitored mixing chamber pressure, and at below 100 Torr, an MKS Baratron unit provided pressure readings to one decimal place. Guest-host mixing ratios of N₂O doped matrices were the ratios of their partial pressures in the mixing chamber. The N₂ and N₂O gas were acquired from Liquid Carbonic, who reported the former to be 99.999% pure, and the latter to be “commercial grade.” The oxygen gas (¹⁶O₂), from Airco Industrial Gases, was reported to be 99.993% pure.

A sensitive needle valve controlled the gas's deposition rate onto the mirror. The substrate was attached with indium to a copper stage cooled by a closed loop helium refrigerator. Temperature was adjustable to 0.1 K increments by varying the current through a $36 \pm 3.6 \ \Omega$ Strip Heater (Minco Company HK12588) with a Digital Temperature Indicator/Controller (Air Products Model ADP-E). The temperature was measured with a Cr/Au thermocouple.

The thermocouple gauge indicated the temperature at the base of the copper cooling finger. The temperature of the actual matrix, frozen onto the substrate attached with indium to the top of the cooling finger, was less than this reading. Comparison of the known O₂ α - β phase transition at 23.8 K, and corresponding shift in matrix isolated O₃ absorbance, with our thermocouple reading when this shift occurred showed the matrix temperature to be within 5 K of the thermocouple gauge reading.⁸

An FT-IR Spectrometer (Nicolet Co., Model 730) equipped with Omnic software recorded transmission spectra. The FT-IR consists of a thermal infrared light source (400 - 5000 cm⁻¹) transmitted through a beam splitter. One of the split beams reflects off of oscillating plane mirror before recombining with the other beam that had reflected off of a stationary plane mirror. As in a Michelson Interferometer, the recombined beams interfere according to the phase difference they acquire after traveling different path lengths.

The recombined beam reflects off the gold mirror substrate to the FT-IR's light detector (Nicolet MCT A Detector Assy, Bias Current 20 mA). Each cycle of the mirror generates a data set $f(\Delta x)$, where Δx is the path length difference. Wavelengths that

constructively interfere at a given Δx satisfy $e^{ik\Delta x} = e^{i2\pi} = 1$, or $\lambda = \Delta x/n$, where n is an integer. The light detector sees transmissions of only certain wavelengths at a particular time. The software which Fourier transforms $f(\Delta x)$ to yield the transmission spectrum $F(\omega)$. Liquid nitrogen cooled the light detector to reduce thermal noise.

The data spacing on the transmission spectrum is 0.241 cm^{-1} , and thus the resolution is 0.5 cm^{-1} . All errors in band location assignments will be this resolution limit of the FT-IR unless otherwise indicated.

A dye laser, pumped by a Lambda Physik Xe-Cl excimer laser, was used to make photogenerated species. The excimer laser emitted 308 nm light from the stimulated emission of $v = 0$ electronically excited xenon-chloride. The laser works in a 3 energy level process. The gas tube consists of approximately 0.1-0.2% HCl gas, 1-9% Xe, the noble gas, and around 90% He, the buffer gas.²⁰

The Xe and HCl gases are in the ground state (1) before a 2300 V potential difference applied across the chamber dissociates HCl into H^+ and Cl^- and ionizes to Xe^+ , to form electronically and vibrationally excited XeCl, state (2). The He buffer gas acquires the vibrational energy upon collision with the XeCl which falls to the electronically excited $v=0$ state (3).²⁰

Since State 2 has a very short lifetime compared to State 3's 10 ns lifetime, many XeCl molecules can occupy State 3 at one time to create a large population inversion. Since XeCl does essentially not exist in the ground state ($\tau \sim 10^{-13} \text{ sec}$), the existence of XeCl denotes a population inversion. Lasing occurs as spontaneously emitted photons resonate in the active medium until they collide with an XeCl to produce other 308 nm photons via the stimulated emission.²⁰

Typical excimer laser power was 150 mJ. The amplified dye laser beam passed through an AutoTracker III frequency doubler, three prisms, and a beam expander before striking the sample. The frequency doubler consisted of a nonlinear uniaxial crystal (one with two frequency dependent indices of refraction). Frequency doubling required orienting the crystal at an angle to the dye laser beam such that the incident and

frequency doubled light encountered the same index of refraction in the crystal. A prism separated the frequency doubled light from the lower energy light. Typical frequency doubled beam power was 30 μJ at 210 nm, 700 μJ at 248 nm.

Experiments

We measured the absorbance spectrum of N_2O isolated in O_2 , N_2 , and mixed matrices (50% N_2 , 50% O_2). The matrices were deposited onto the mirror at a vacuum chamber pressure of 2×10^{-6} Torr and thermocouple reading $T = 11$ K. The second "Herzberg matrix" irradiated with 248 nm light was deposited at $P = 2 \times 10^{-5}$ Torr in an attempt to increase N_2O yield. Since deposition time for this matrix was half that of the first Herzberg matrix, this second Herzberg matrix was five times as thick as the first one, assuming a linear thickness increase with deposition time.

All absorbance spectra were generated from the FT-IR transmission spectra using Lambert-Beer's Law:

$$I_t = I_o e^{-N\sigma x} = I_o e^{-\mu x},$$

where N is the absorbing sample's particle density, σ its absorption cross section and x its thickness. The exponential term μ is the *optical density* of the matrix, and has units of inverse distance.²¹ The background spectrum, I_o , was measured before matrix deposition for the matrix isolation experiments, and before irradiation for the photogeneration experiments.

The *penetration depth* x_c , of the matrix is the distance light can travel in the matrix before it's intensity drops to $\frac{1}{e}$ of its initial value. From Lambert-Beer's Law, we see that $x_c = \frac{1}{N\sigma}$. To calculate x_c for at 248 nm for a mixed N_2/O_2 matrix, we can ignore N_2 absorptions because at 248 nm, as $\sigma < 10^{-26}$ m^2 for N_2 ,²² while $\sigma \sim 10^{-25}$ m^2 for O_2 .⁴ From matrix data given above, the O_2 number density N is on the order of 10^{-2} molecules/ \AA^3 , which yields a penetration depth of $x_c \sim 1$ mm, a distance much greater than a typical matrix thickness, 1 μm .⁸ Hence the laser penetrated all the matrices, including the second "Herzberg" matrix.

The FT-IR and Omnic program generates a transmission spectrum, i.e., $I_t(\text{cm}^{-1})$ and $I_o(\text{cm}^{-1})$. We generated an absorption spectrum by solving Lambert-Beer's Law for μx . Since liquid N_2 evaporation decreased the light detector's sensitivity, the background spectrum was aligned with transmission spectra taken at later times before generating absorption spectra.

IV. Results

Table 1 shows the matrix shifts and the band widths (FWHM) of N_2O 's fundamental vibrational modes. Emphasized is data revealing the nature of N_2O in the matrix environment.

Table 1: Matrix Shifts / Bandwidths of Fundamental Vibrational Modes of Matrix Isolated N_2O (1 N_2O /760 host molecules)

vibrational transition from ground state	Gas Phase ²³ / cm^{-1}	N_2 matrix ²⁴	N_2 matrix (this paper)	O_2 matrix	N_2/O_2 matrix ($\text{N}_2:\text{O}_2 \approx 1:1$)	Ar matrix ²⁴
$\nu_1: 100$	1285.0	+ 6.2	+ 6.1/1	+ 1.0/1; - 1.6/1	+ 5.9/1.2	+ 2.3 - 2.1
$\nu_2: 010$	588.8	- 0.8	- 0.8/0.5	- 1.8/0.5 + 2.0/0.8	--	- 0.6 - 1.8
$\nu_3: 001$	2223.5	+ 11.6 + 9.5	+ 11.8/1 + 9.5/1	- 4.1/1 - 1.2/1	+ 11.8/1 + 9.5/1	+ 3.5 - 5.2
peak height ratio $\nu_1:\nu_2:\nu_3$	1.0:.012:5.8 (²⁵)	--	1:0.032:2.16	1:0.2:16.2	1:0.4:2.64	--

Matrix Isolated N_2O

- In N_2 Matrices

Nitrous oxide's stretching modes (ν_1 and ν_3) in the N_2 matrix are blue shifted by ~0.5% of the gas phase value. Band widths for the stretching modes are close to 1 cm^{-1} , while those for the much weaker bending mode are between $0.5\text{-}0.8 \text{ cm}^{-1}$. Figure 4.1a shows absorbance bands corresponding to the ν_3 mode at 2235.3 cm^{-1} and 2233.0 cm^{-1} . While neither Smith and Overend (1972) nor H. Bahou et al (1997) did not detect the 2233.0 cm^{-1} band, Nxumalo et al. (1994) found the same doublet we did, with the higher

energy band being the stronger of the two absorptions^{25, 26, 24}. Figure 4.2b shows the ν_1 absorbance of N_2O in the N_2 matrix at $\text{MR} = 1/760$.

The two dilute matrices contain two other sets of doublets separated by 2.3 cm^{-1} , Figure 4.1b. They are $1/100$ as strong as the strongest ν_3 band. The larger bands, both blue shifted by 2.3 cm^{-1} , are at 2213.08 cm^{-1} and 2189.05 cm^{-1} . Smith and Overend (1972) report ν_3 of $^{14}\text{N}^{15}\text{N}^{16}\text{O}$ and $^{15}\text{N}^{14}\text{N}^{16}\text{O}$ to be 2189.4 cm^{-1} and 2213.5 cm^{-1} respectively.²⁶ Since these findings are comparable to ours, shown in Figure 4.1b, we can similarly identify the presence of $^{14}\text{N}^{15}\text{N}^{16}\text{O}$ and $^{15}\text{N}^{14}\text{N}^{16}\text{O}$ in the matrix at one hundredth the concentration of $^{14}\text{N}^{14}\text{N}^{16}\text{O}$.

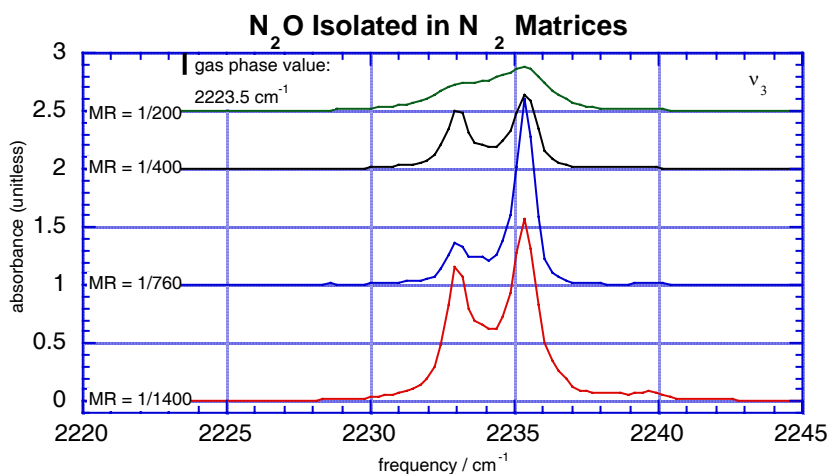


Figure 4.1a: Asymmetric stretch absorption of N_2O isolated in an N_2 matrix is blue shifted from its gas phase value by 12 cm^{-1} .

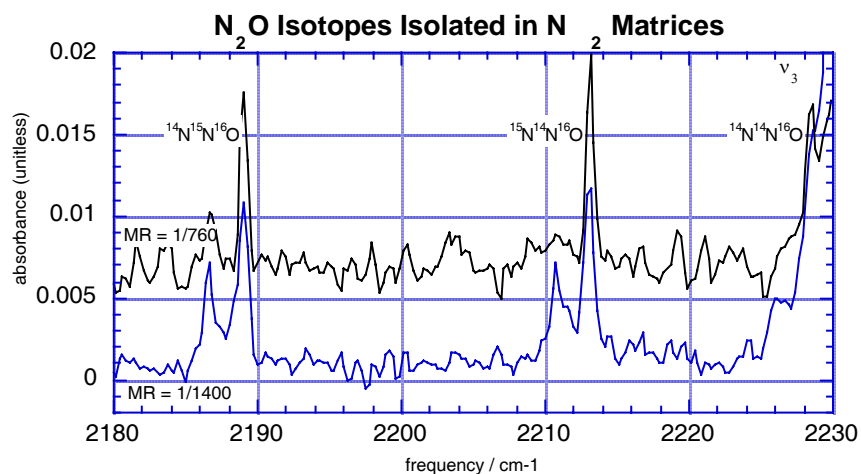


Figure 4.1b: Asymmetric stretch absorptions of N_2O isotopes isolated in an N_2 matrix.

- In O_2 Matrices

Each of N_2O 's vibrational modes appear as doublets in the O_2 matrix environment. The ν_1 and ν_2 doublets straddle their respective gas phase values. Both ν_3 peaks are red shifted, as shown in Figure 4.2a. One peak of the ν_3 doublet, at 2219.5 cm^{-1} , is red shifted by $\sim 0.2\%$ from the gas phase value. The other ν_3 peak is less red shifted, at 2222.3 cm^{-1} .

At high N_2O concentration, $\text{MR}=1/380$, the ν_3 doublet has a shoulder extending to 2240 cm^{-1} . In the shoulder there are two weak peaks (2224 cm^{-1} and 2232 cm^{-1}) corresponding to small absorbance bands visible in the $\text{MR}=1/760$ spectrum.

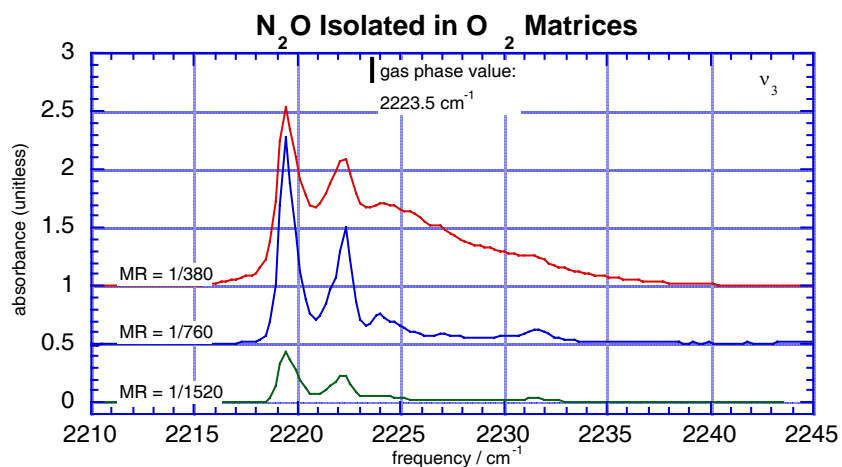


Figure 4.2a: The asymmetric stretch of N₂O isolated in an O₂ matrix is red shifted from its gas phase value by 4 cm⁻¹.

- In Mixed N₂+O₂ Matrices

The v₃ absorbance of N₂O lightly doped in a mixed matrix (MR=1/1520) is indistinguishable from its absorbance in an N₂ matrix of the same MR, as shown in Figure 4.3a. At high concentration, MR=1/152, the v₃ absorbance band broadens and is red shifted. There is significant absorbance in the 2220-2230 cm⁻¹ range, the frequency range the v₃ band of N₂O isolated in an O₂ matrix.

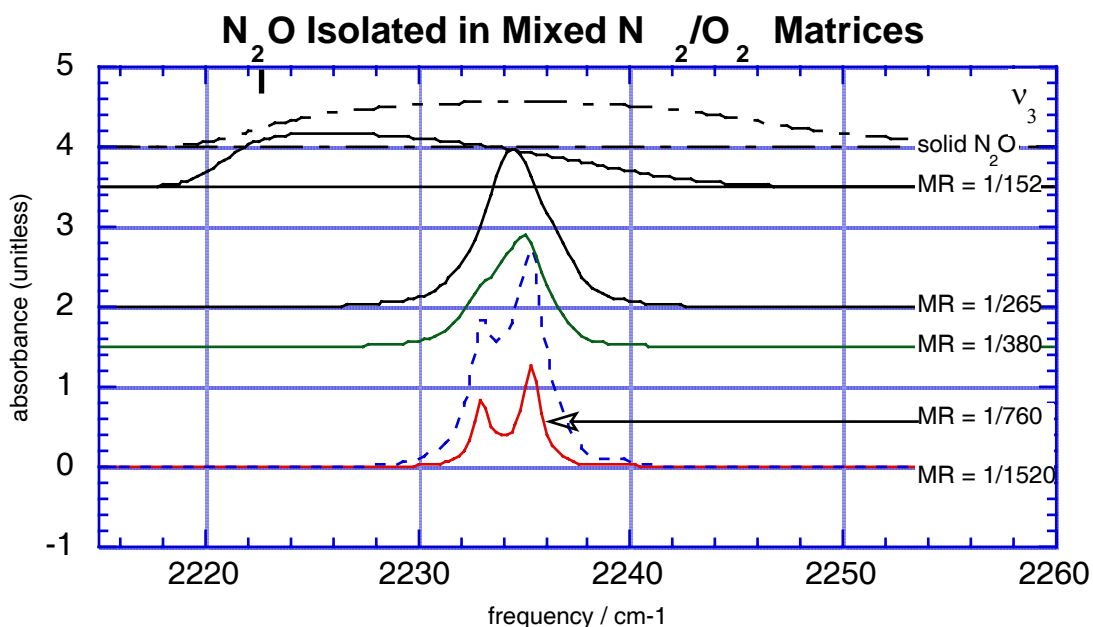


Figure 4.3a: The asymmetric stretch absorption of N_2O isolated in an N_2/O_2 matrix is blue shifted from its gas phase value, 2223.5 cm^{-1} , by 11 cm^{-1} .

The ν_1 mode of N_2O in the mixed matrix is centered at 1290.9 cm^{-1} , as shown in Figure 4.3b. While its peak is very close to that of the ν_1 absorbance of N_2O in the N_2 , the line width is 20% larger. While the "feet" of the band extends into the region of the O_2 matrix doublet ($\nu_1 = 1286\text{ cm}^{-1}$), there is no peak in the mixed matrix absorbance band corresponding to it.

Symmetric Stretch Mode Absorbance of Matrix Isolated N₂O

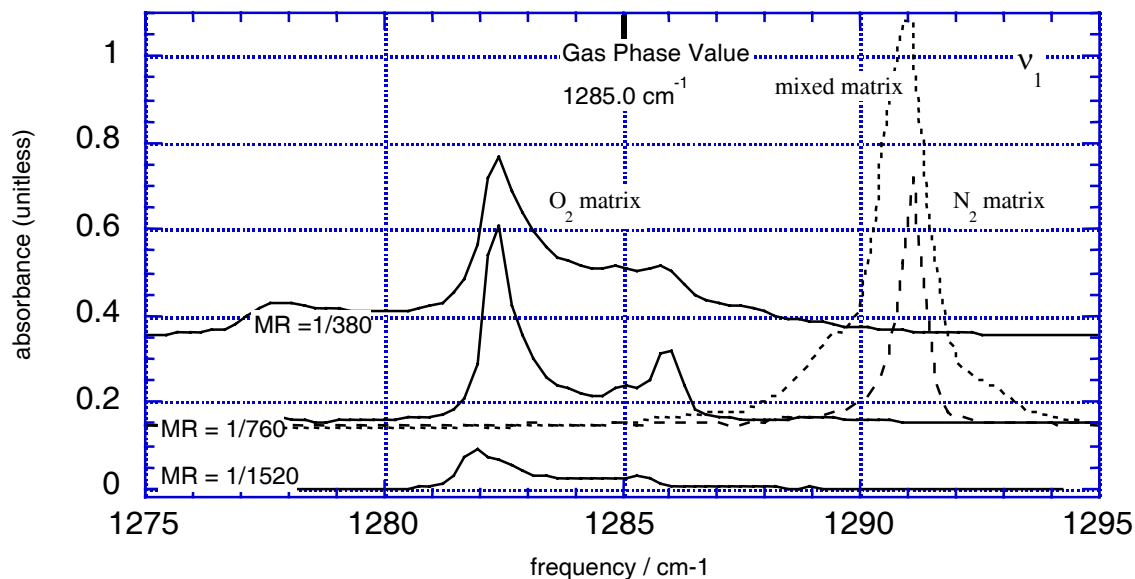


Figure 4.3b: N₂O's symmetric stretch absorption is blue shifted in N₂ and mixed matrices and red shifted on O₂ matrices.

Irradiated N₂:O₂ Matrices: O₂ + hν(248nm) → O₂^{*}(H)

- ν₃ Absorbance

Irradiation of a mixed matrix (N₂:O₂=1:1) with 248 nm light yielded absorbance bands corresponding to both the ν₃ mode of O₃ and N₂O in two mixed matrices. The first was deposited at the normal rate (see Section III) and was irradiated with 600 J. The ν₃ peak for N₂O was 10.3 cm⁻¹ wide and centered at 2230.0 cm⁻¹, as shown in Figure 4.4. This absorbance band is red shifted from ν₃ peak of N₂O doped in a mixed matrix.

The second matrix, deposited at ten times the rate as the first matrix and for half the time, was irradiated with 60 J. The photogenerated N₂O in this thick matrix was 7.3 cm⁻¹ wide and centered at 2229 cm⁻¹.

Matrix isolated ozone absorption, ν₃ = 1038 cm⁻¹, agrees with past matrix isolation studies.²⁷

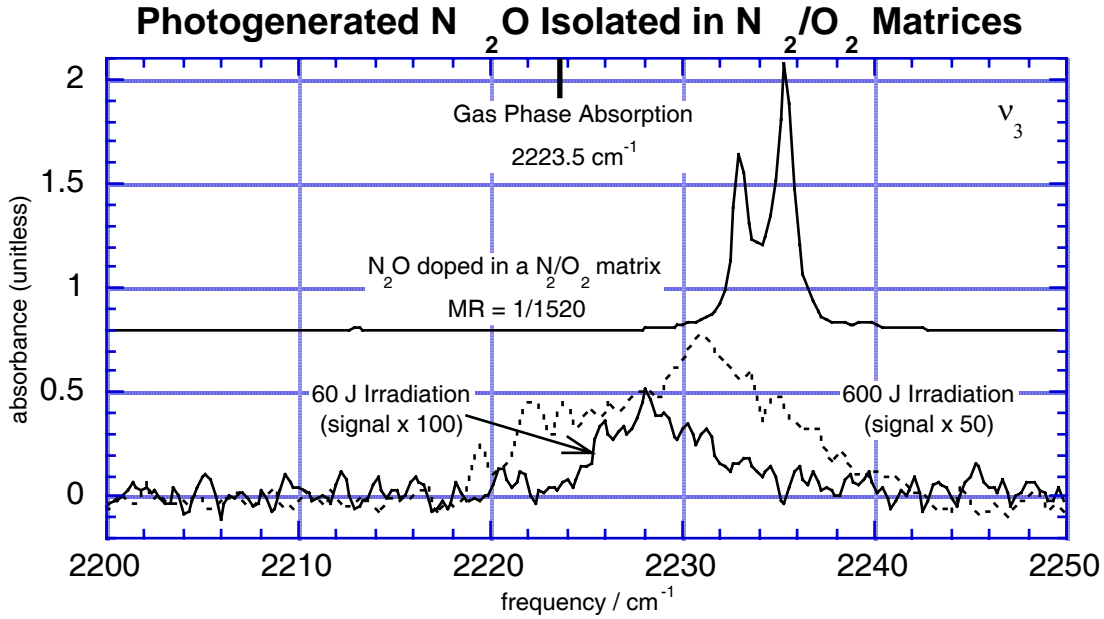


Figure 4.4a: Photogenerated N_2O (248 nm) in a mixed matrix. The NO absorption band overlaps those of N_2O doped in N_2 matrices, O_2 matrices, and mixed N_2/O_2 matrices.

- Growth Curves

Figures 4.4b and 4.4c show the growth curves for photogenerated N_2O and O_3 in the thin and thick matrices respectively. Irradiation dose is the product of the energy per laser pulse, the duration of irradiation, and the laser pulse frequency, 10 Hz. The absorbance, μx , of each matrix is the product of its optical density, μ (m^{-1}), and its thickness, x (thin), or X (thick). The error bars were calculated by assigning an uncertainty in $\Delta I_t = \Delta I_o = 0.02$, in transmission units used in the FT-IR software, and adding the errors in absorbance in quadrature:

$$\sigma_{\mu x} = \sqrt{\left(\frac{\partial \mu x}{\partial I_o} \Delta I_o\right)^2 + \left(\frac{\partial \mu x}{\partial I_t} \Delta I_t\right)^2} = \sqrt{\left(\frac{\Delta I_o}{I_o}\right)^2 + \left(\frac{\Delta I_t}{I_t}\right)^2},$$

where μx , I_o , and I_t are related by Lambert-Beer's law.

We fit both N_2O growth curves to a line in order to compare growth rates at initial irradiation doses (< 60 J), and greater doses. N_2O generation from the bimolecular process insures that the growth curve slope at small irradiation, Figure 4.4c, is smaller than the slope at large doses, Figure 4.4b.

Since there were too few data points in Figure 4.4b (~1 point per 25 J) to measure an increasing growth rate, we deposited the thick matrix and recorded spectra between irradiation intervals of just above 1 J.

Matrix Isolated N₂O and O₃ Absorbance as a Function of Irradiation Dose

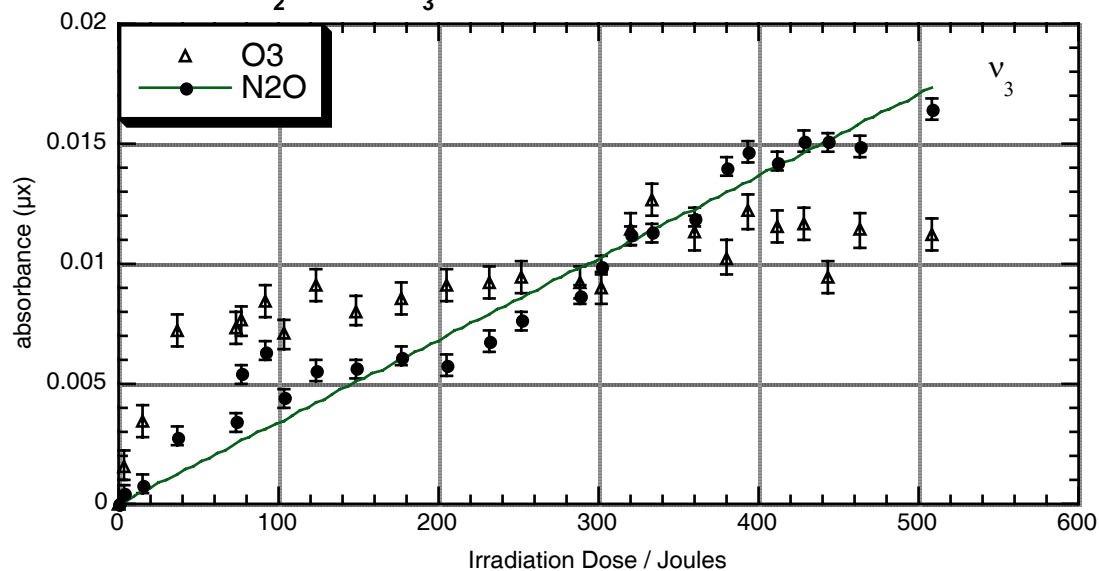


Figure 4.4b: To a first order fit, photogenerated N₂O concentration increases at $(3.42 \pm 0.08) \times 10^{-5} \text{ J}^{-1}$.

Matrix Isolated N₂O and O₃ Absorbance as a Function of Irradiation Dose (<60 J)

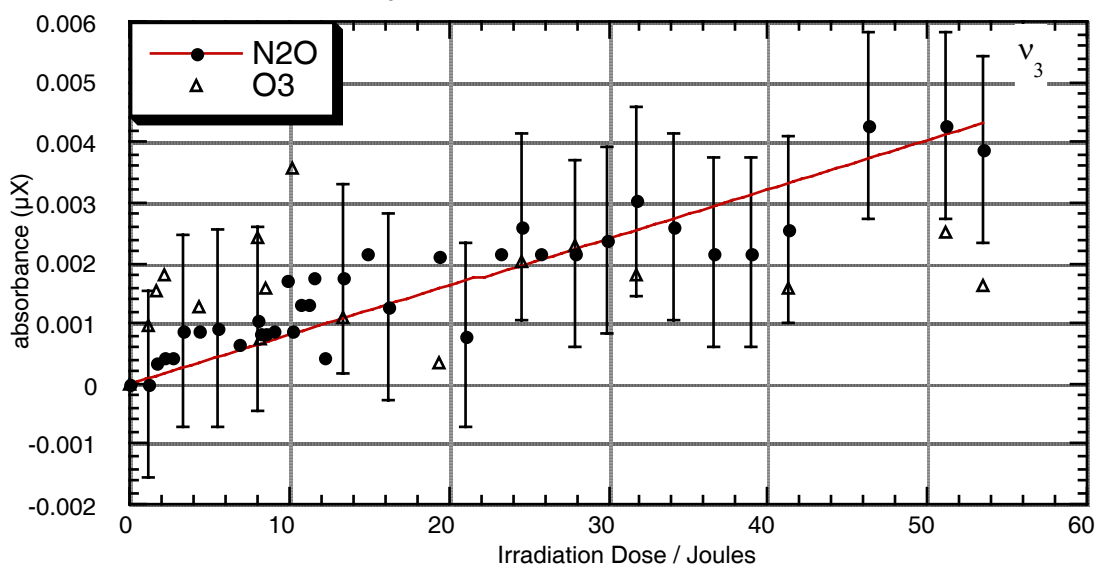


Figure 4.4c: The N₂O concentration increases at $(8.0 \pm 0.4) \times 10^{-5} \text{ J}^{-1}$ at irradiation doses less than 60 J. Portions of error bars extending to $\mu\text{X} \leq 0$ have no physical significance.

While keeping matrix thickness constant would better isolate variables, depositing a thick matrix was necessary to ensure that we did produce N₂O. Experiments done in attempt to replicate the data in Figure 4.4b, with more data points at small irradiation doses, failed to produce N₂O. We believed that either the laser beam was not completely hitting the substrate, or that there was no matrix on the mirror to irradiate prevented N₂O production. Due to limited beam time, we realigned the laser and deposited a thick matrix to ensure that N₂O was formed.

While the absorbance values at irradiation doses less than 60 J are comparable in both matrices, the nature of the laser beam makes accurate comparison of growth curves difficult. The matrix was irradiated with frequency doubled laser pulses expanded with lenses to irradiate the entire matrix. The light pulse was not a uniform circle, at the vacuum chamber entrance, but rather a ring of light around a circular light patch.

During irradiation, the pulse energy would fall from an initial maximum value as the components of the lasers and frequency doublers heated up. A pulse energy, the average of the energy measured before and after each irradiation dose, was assigned to each spectrum taken. These energies generated the x-axis of the growth curves.

While spectra were taken, the orientation of the frequency doubling crystal with respect to the beam path was adjusted to keep pulse energy constant during irradiation. This adjustment changed where the beam hit the mirror. Since the beam was not uniform, the beam shift changed the amount of energy the matrix absorbed during the times recorded between data measurements.

V. Discussion

Matrix Isolated N₂O

- Blue Shifts

Nitrous oxide's stretching modes in the N₂ matrix are blue shifted by ~0.5% of the gas phase value. Smith and Overend investigated matrix isolated N₂O and tried to predict matrix shifts by changing N₂O's potential energy function.²² They represented

the effects of the matrix “cage” on N₂O's vibrational modes by adjusting N₂O's quadratic force constants. These are coefficients of second order terms of the intra-molecular potential energy function, or the forces constant of harmonic oscillators. Hence, N₂O isolated in an N₂ matrix can be modeled as a one-dimensional harmonic oscillator, Figure 5.1.

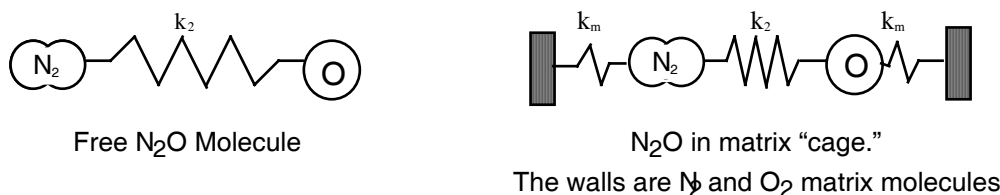


Figure 5.1 a) N₂O in the gas phase. Considering only the N₂--O bond, and hence the ν_1 band,*

the N₂O vibrates at $\nu_1 = 2\pi\sqrt{\frac{k_2}{m}}$, where m is N₂O's mass. b) The matrix cage, to the left and right of the linear N₂O, exerts a force on the ends of the molecule, which is represented by

springs with spring constant k_m . The matrix isolated N₂O vibrates at $\nu_1 = 2\pi\sqrt{\frac{k_2+2k_m}{m}}$, faster than the gas phase N₂O.²⁸

- N₂+O₂ Matrix

The similarities of spectra of N₂O doped in N₂ matrices and mixed matrices suggest that the N₂O in the mixed matrix is in an N₂ environment. Since there was no absorbance in the mixed matrix corresponding to N₂O in an O₂ matrix (2118 cm⁻¹, 1286 cm⁻¹), virtually all N₂O isolated in a mixed matrix must be surrounded by N₂ in the matrix. This indicates that while the gas deposited on the mirror was mixed homogeneously, the matrix was not. The heterogeneous gas froze into a matrix containing homogenous regions of N₂ and O₂; the N₂O froze in N₂ regions.

* L.M Nxumalo et al. (1994) attribute the ν_1 absorption to the vibration in the NO bond, and the ν_3 band to vibration in the NN bond of N₂O because their “ab initio calculations of the normal coordinates of the nitrous oxide monomer show quite clearly that the fundamental vibration is localized almost exclusively” in these bonds” Details most likely reside in their other paper, L.M Nxumalo et al., *J. Mol. Struct. (Theochem)*, 307, 153, 1994.²⁴

Since O₂ has a higher melting point than N₂, it is not likely that only the N₂ and N₂O were frozen onto the mirror. A typical N₂ matrix would leave the mirror, or "blow off" at a T = 25 K, while an O₂ matrix would stay on the mirror at temperatures below 30 K. A large increase in vacuum chamber pressure accompanying a temperature increase indicates that much of the matrix material has come off the mirror.

Differences in vibrational frequencies in photogenerated and N₂O doped in N₂ matrices, which we also found (reported below), motivated M. Bahou et al. (1997) to look at N₂ doped in mixed matrices. They reported a difference in vibrational spectra of N₂O in N₂ matrices (MR = 1/1000) and N₂O/O₂/N₂ (MR = 1/6/1000 and 1/12/1000) matrices. In the mixed matrices, they assign an absorption at $\nu_1 = 1290.4 \text{ cm}^{-1}$ and $\nu_3 = 2235.0 \text{ cm}^{-1}$ to a N₂O...O₂ van der Waals complex, which increases with O₂ concentration. Their corresponding N₂O monomer bands were $\nu_1 = 1291.2 \text{ cm}^{-1}$ and $\nu_3 = 2235.55 \text{ cm}^{-1}$.²⁵ If such species existed in our matrices, their absorbance bands were buried in the feet of our monomer peaks at $\nu_1 = 1291.1 \text{ cm}^{-1}$ and $\nu_3 = 2235.3 \text{ cm}^{-1}$. Further, the spacing between the N₂O monomer and complex absorptions is close to the resolution limit of our spectrometer, 0.5 cm⁻¹, and hence we could not easily distinguish the two bands.

- Red Shifts

N₂O's ν_3 band are red shifted by ~0.2% in the O₂ matrix environment. Again modeling the N₂O as a ball and spring system, the red shift indicates that O₂ matrix environment decreases the spring constants, or weakens bond strengths, of the N₂O.

As seen in Table 1, N₂O bands red shift in an argon matrix as it does in an O₂ matrix. Sodeau and Withnall used a MR = 1:10⁴ mixing ratio and measured spectra at 4.2 K.² N₂O in a xenon matrix (MR = 1:729, T = 32 K) absorbed at $\nu_3 = 2214.5 \text{ cm}^{-1}$.²⁹

There is a correlation between the number of molecules per matrix unit cell and the type of matrix shift they induce N₂O's vibrational modes. Xe, Ar, and O₂ matrices all

contain one molecule per unit cell and induce similar red shifts on N₂O. The N₂ matrix has four molecules per unit cell and in it, N₂O's vibrational modes are blue shifted.

The differences in molecules per matrix unit cell translate into differences in matrix number densities. The number densities for the Ar and Xe matrices are 6.68 molecules/nm³ and 4.34 molecules/nm³, respectively.¹⁸ The rare gas matrix number densities are closer to that of the α -O₂ matrix, 14.4 molecules/nm³, than of α -N₂, 22.1 molecules/nm³. Further investigation of these correlations may lead to a good explanation of why a matrix induced a red or a blue shift on N₂O.

Another means of explaining different matrix shifts is to compare the ratios of vibrational mode absorptions. Gas phase peak height ratios, $\nu_1:\nu_2:\nu_3=1.0:0.12:5.8$,²⁵ are valuable in assessing the effects of N₂ and O₂ on the stretching modes. As shown in Table 1, the $\nu_3:\nu_1$ peak height ratio in the O₂ matrix is eight times that of the ratio in the N₂ matrix. This difference indicates that the effect of matrix environment on N₂O absorption cross section is frequency dependent. There may be a correlation between the ν_3 red shift and this vibrational frequency's strong absorption in the O₂ matrix.

• Doublet Absorptions

The effect of a matrix on different modes also manifests itself in doublet absorptions. All three N₂O vibrational modes in the O₂ matrix are doublets while only the ν_3 mode is a doublets in the N₂ matrix.

The two peaks in a doublet may correspond to different types orientations the N₂O has in the matrix. A molecule in an *interstitial site* is located in the space of the lattice. A molecule in a *substitutional site* is located at a lattice site, i.e., it replaces a matrix molecule in the lattice. The substitutional hole in N₂ is 3.99 Å and in O₂, 3.64 Å.¹⁸

If site differences explain doublets, the frequencies of all three modes of an N₂O in an O₂ matrix depend on the type of site the N₂O occupies. Yet this implies that while the ν_1 and ν_2 mode of N₂O isolated in an N₂ matrix are not effected by the type of site

the N₂O occupies, the ν_3 mode is site dependent. This seems implausible because if one stretching mode is site dependent, the other would be, too.

Soudeau and Withnall attribute the breaking of degeneracy as causing the N₂O ν_2 doublet they observed in an argon matrix (Table 1).² A matrix site lacking this spherical symmetry can break a degeneracy. In a spherically symmetric potential, an N₂O molecule vibrates at eigenfrequencies of both the Hamiltonian and the parity operator.

Modeling the molecule as a ball and spring system, with the central N at the origin of the coordinate system, helps explain symmetry breaking. An N₂O molecule in a spherically symmetric substitutional matrix site is analogous to the ball and spring system in a spherical cage centered about the origin. It vibrates the same way before and after operating with the parity operator, which in this case means switching the positions of the end atoms by pulling them through the origin and out to their initial radial distances from it. Rotating the molecule 180° about the origin achieves the same result. There are no physical differences between the two states because the cage has spherical symmetry.

A matrix site lacking spherical symmetry can be modeled by either displacing the center of the spherical cage from the central atom of N₂O, or by denting one side of the cage. If in the initial state, $|1\rangle$, the O is closer to the cage than the end N atom, then after using the parity operator, the final state, $|2\rangle$, has the O further from the cage than the N, and the forces on the N₂O in states 1 and 2 are different.

N₂O molecules in a matrix containing nonspherical matrix sites are trapped in one of these two states, and hence vibrate differently. As shown in Figure 1.1, the equilibrium bond lengths of N₂O add to more than half the diameter of the N₂ and O₂ matrix substitutional holes.

Raising the temperature of the matrix can test the stability of the doublet sites. Since the matrix was deposited from room temperature gas, it is possible that it froze as a heterogeneous lattice. N₂O embedded in such a lattice could have different environments that induce different matrix shifts. The process of *annealing* the matrix, slowly warming

it up and cooling it down, can make the matrix more uniform as the matrix molecules can arrange themselves in positions of lowest energy when the temperature decreases slowly in time. The doublets in the N₂ matrix, as well as those in the O₂ and mixed matrices, remained after annealing at 22 K, 30 K, and 22 K, respectively.

- N₂O Dimer and Aggregate identification

N₂O aggregates are most visible in the O₂ matrices. The shoulder to the higher energy side of the ν_3 doublets in the high concentration N₂O sample is the absorbance of N₂O aggregates. The peaks at 2223.6 cm⁻¹ and 2231.4 cm⁻¹, most prominent in the MR = 1/760 spectrum, may be (N₂O)₂. The difference between the MR 1/760 and MR 1/380 shows that at higher mixing ratios, the number of adjacent N₂O molecules increase, the dimer concentration increases, as well as multimers and larger N₂O clusters. The presence of two sets of doublet bands indicate that both N₂O monomers and dimers can occupy two different lattice sites. These sites correspond to the two sites the individual N₂O molecules occupy in the low MR matrices. The lower energy peak of the ν_3 doublet in the N₂ matrix, Figure 4.1a, may also be a dimer. Neglecting the spectrum of the MR=1/1400 matrix, this band increases in intensity as MR increases. Irradiating the doped O₂ matrices to dissociate the N₂O can test the dimer identification hypothesis, as (N₂O)₂ concentration decreases faster than N₂O concentration when the matrix is irradiated with 189 nm light.²

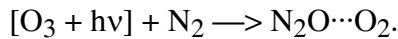
Nxumalo and Ford identify absorptions at 1285.7 cm⁻¹ and 2239.7 cm⁻¹ to increase similarly upon annealing the matrix (deposited at 17 K) to 35 K. Upon annealing, the ν_1 and both ν_3 doublet absorptions decreased similarly. They conclude that these absorptions are those of N₂O dimers, which consist, based on predicted absorbance frequencies, of two N₂O monomers with aligned dipole moments antiparallel such that the four N atoms form a rectangle.²⁴ The corresponding decrease in the main absorbance bands makes their dimer identification convincing and confirms that the doublets correspond to N₂O in different types of lattice sites. As noted above, I did

not observe decreased absorbance upon annealing my matrices. Yet, I did not observe that the bands *did not change* either, but only if they still existed after annealing. This is definitely motivation to check the data, though I do not have access to it now.

Irradiated N₂:O₂ Matrices: $O_2 + h\nu_{(248\text{ nm})} \rightarrow O_2^*(H)$

- Matrix Shifts

The ν_3 band of photogenerated N₂O in a mixed matrix (2229, 2230 cm⁻¹) was red shifted (5-6 cm⁻¹) from the absorbance bands of N₂O doped in a mixed matrix. Since the photogenerated N₂O was formed from the interaction of matrix hosts N₂ and O₂, its local environment must contain *both* N₂ and O₂. The heterogeneous matrix environment places the ν_3 absorption band between those of N₂O doped in O₂ and N₂ matrices. This conclusion is similar to that of M. Bahou et al., discussed above. They claim the N₂O formed in the bimolecular process forms an N₂O···O₂ van der Waals complex:



The photogenerated N₂O bands correspond with the doublet band in their doped matrices that they assign to the above complex.²⁵

The signal to noise ratio for the ν_3 band was 4:1. The small ratio explains the absence of the ν_1 and ν_2 bands, which were 1/3 and 1/60 as strong as the ν_3 band in the N₂O doped mixed matrix.

- Growth Curves

Figure 4.4c shows the growth of N₂O and O₃ at small irradiation doses. Assuming a linear growth of matrix thickness with deposition time, the thick matrix of Figure 4.3c is five times as thick as that of Figure 4.3b, i.e., $X = 5x$. If the matrices were the same thickness, a slope comparison would show whether N₂O grew in linearly.

Since we have matrices of different thickness, we must look at μ , the optical density (m⁻¹), rather than the unitless absorbance. The optical density as a function of irradiation dose, Ir , is the same for both matrices. Setting the thin matrix thickness to

$x=1$, we must divide the slope of the line in Figure 4.3c by $5x = 5$ to compare slopes.

This yields an N_2O growth rate $\frac{\partial\mu}{\partial I_{low}} \approx 1.6 \times 10^{-5} \text{ J}^{-1}$, which is nearly half the growth rate of N_2O at higher irradiation doses (60-600 J), $\frac{\partial\mu}{\partial I_{high}} \approx 3.4 \times 10^{-5} \text{ J}^{-1}$.

We can not conclude, due to the large error bars in Figure 4.4c, that the growth rate increased. That three-quarters of the data points are above the plotted line indicates that $\frac{\partial\mu}{\partial I_{low}} \geq 1.6 \times 10^{-5}$. Large signal to noise ratios lend an inherent inaccuracy to measurement of small absorptions. Even if we could measure absorbances more accurately, we would still encounter difficulties in distinguishing from N_2O formed directly and indirectly because the composite growth curve is nonlinear. We would need to compare a more accurate version of the above growth curves to N_2O growth curves involving formation by the bimolecular process only.

Upon initial inspection, we considered a control matrix irradiated with light just strong enough to dissociate O_2 , i.e., $\lambda \approx 240 \text{ nm}$. Yet, O_3 made by this process differs from O_3 made from $\text{O}_2^*(\text{H})$, so this type control matrix would involve changing variables other than $\text{O}_2^*(\text{H})$ formation. The other option is to irradiate a control matrix with light not lacking the energy, rather than have too much energy, to excite O_2 to $\text{O}_2^*(\text{H})$.

- Future Research

The best way to distinguish N_2O formed from O_3 dissociation products and N_2O possibly made from $\text{N}_2 + \text{O}_2^*$ is to begin with an O_3 doped mixed N_2/O_2 matrix. This control matrix (I) will be irradiated with " λ_{H} ," which will dissociate O_3 but will not excite the O_2 's from dissociated O_3 to $\text{O}_2^*(\text{H})$. The test matrix (II) will be irradiated with $\lambda = 248 \text{ nm}$ light. Such irradiation will dissociate O_3 and excite the O_2 dissociation products to $\text{O}_2^*(\text{H})$.

While N_2O will be formed via the bimolecular process in both matrices, and $[\text{O}_3]$ will decrease as $[\text{N}_2\text{O}]$ increases. The $\text{O}(^1\text{D})$ from dissociated O_3 that do not form N_2O

will lose their kinetic energy to the matrix environment and become unbound $O(^3P)$.²⁸ Now consider how $N_2 + O_2^*(H) \rightarrow N_2 + O$, if the reaction happens, effects these growth and decay curves: If N_2O is a sink for $O_2^*(H)$, then O_3 will decay more quickly in matrix II than matrix I, as N_2 and O_2 will compete for the $O_2^*(H)$. In the presence of N_2 , some $O_2^*(H)$, instead of forming O_3 , may form N_2O .

The wavelength, λ_H , in the control experiment should be as close to 248 nm as possible to minimize differences in absorption cross sections at the different wavelengths. Yet, this light must not be strong enough to excite O_2 to $O_2^*(H)$. We can determine this wavelength experimentally by looking for the ν_3 band of O_3 in an irradiated undoped N_2/O_2 matrix. Starting at $\lambda > 310$ nm, which excites O_2 to the lowest level of the $O_2^*(c)$ state, we decrease irradiation wavelength until O_3 is detected. The longest wavelength in which O_3 is detected will be λ_H . At shorter wavelengths, $O_2^*(H)$ is formed and may form N_2O .

The quantum yield of (2.10b) places an upper limit on the maximum of λ_H , as above $\lambda \approx 302$ nm, $O(^1D)$ does not form from O_3 photodissociation. In this wavelength region, $\sigma \sim 10^{-23}$ m² for O_3 , while at 248 nm, $\sigma \sim 10^{-21}$ m².¹¹ Hence, $[N_2O]$ will increase faster and $[O_3]$ decrease faster in matrix II than I because of the large wavelength dependence in O_3 absorption cross section. More O_3 is dissociated at $\lambda = 248$ nm than at longer wavelengths. Normalizing the irradiation dose to the matrix can compensate for the wavelength dependence of σ . As long as the test and control matrices are the same thickness, x , we can plot

$$Nx = \frac{1}{\sigma(\lambda)} \ln\left(\frac{I_t}{I_o}\right),$$

as this follows from Lambert-Beer's law.

Photogenerated N_2O may absorb differently based on how it was formed. If N_2O formed in the bimolecular process forms the $N_2O \cdots O_2$ complex, as claimed by M. Bahou et al., and direct N_2O formation from $O_2^*(H)$ does not, then we need not compare growth curves at all, but only at the frequencies of N_2O absorbance bands in our test and control matrices.

Conclusions

The fundamental vibrational mode frequencies of N₂O isolated in an N₂ matrix are blue shifted while those in an O₂ matrix are red shifted. When an equal mixture of room a temperature N₂ and O₂ encounters a substrate of 10 K, the N₂ and O₂ separate upon freezing, and small amounts of N₂O in the gas congregates around the N₂.

Due to large signal to noise ratios and the O(¹D) source of N₂O, we could not determine from the N₂O growth curves whether $N_2 + O_2^*(H) \rightarrow N_2O + O$. A comparison of photogenerated N₂O growth and O₃ decay curves in O₃ doped mixed matrices can distinguish between the bimolecular N₂O formation and a combination of bimolecular and direct N₂O formation from O₂^{*}(H). The test matrix is irradiated to dissociate O₃, excite O₂ to O₂^{*}(H). The control matrix is irradiated at a longer wavelength that dissociates O₃ while not creating O₂^{*}(H). Comparison of N₂O absorbance bands in the test and control matrices might also be fruitful.

Acknowledgments

This work would not have been possible without the following people at SRI International: Dr. Philip Cosby and Dr. Jay Jeffries for accepting me to SRI's Research Experience for Undergraduates program; Dr. Richard Copeland for his supervision; Dr. Christian Bressler for showing me the ropes, his guidance and probing questions; and Dr. Hannelore Bloemink and Dr. Eunsook Hwang for helping with the dye laser and frequency doubler. Thanks also to Dr. Tom Donnelly at Swarthmore College for helping me smooth out rough drafts of this document.

Literature Cited

- ¹ T. Machida, et al. *Geophys. Res. Let.*, 22, 2921, 1995.
- ² J. R. Soudeau and R. W. Withnall, *J. Phys. Chem.*, 89, 4484, 1985.
- ³ R.P. Wayne, *Chemistry of Atmospheres*. Oxford, Clarendon Press, 1985.

- 4 H. Okabe, *Photochemistry of Small Molecules*. New York, John Wiley & Sons, 1978.
- 5 B.J. Finlayson-Pitts and J.N. Pitts, *Atmospheric Chemistry*. New York, John Wiley & Sons, 1986.
- 6 M. Dubey, personal Correspondence, SRI International.
- 7 T.G. Slanger and P.C. Cosby, *J. Phys. Chem.*, 92, 267, 1988.
- 8 C. Bressler, personal correspondence, SRI International.
- 9 R. A. Copeland, Knutsen, Slanger, *Proceedings of the International Conference on Lasers '93*. McLean Virginia, STS Press, 1994.
- 10 R.A. Copeland and T.S. Slanger, Proposal to the National Science Foundation: "O₂ Herzberg State Reaction with N₂ — A Possible Source of Stratospheric N₂O," 1995.
- 11 Hay et. al., *J. Phys Chem.* 86, 862 1982.
- 12 B. Buijsse, E.S. Hwang, T.G. Slanger, H. Riris, C.B. Carlisle, and R.A. Copeland, "Upper Limit for the Production of N₂O from the Reaction of O₂(A³Σ_u⁺) with N₂," in preparation.
- 13 L. Brown and V. Vaida, *J. Phys. Chem.* 100, 7849, 1996.
- 14 DeMore and Davidson, *J. Phys. Chem.* 34, 5869, 1959.
- 15 F. Daniels and R. Alberty, *Physical Chemistry*, 4th ed. New York, John Wiley & Sons, 1975.
- 16 M. L. Boas, *Mathematical Methods in the Physical Sciences*, 2nd ed. New York, John Wiley & Sons, 1983.
- 17 E.C. Zipf and S.S. Prasad, *Nature*, 295, 133, 1982.
- 18 H.J. Jodl, Solid-State Aspects of Matrices, *Chemistry and Physics of Matrix Isolated Species*. L. Andrews and M. Moskvits, eds, 343, 1989.
- 19 C.S. Barret, L. Meyer, and J. Wasserman, *J. Chem. Phys.* 47, 592, 1967.
- 20 P.W. Millonni and J.H. Eberly, *Lasers*. New York, John Wiley & Sons, 1988.
- 21 R.A. Day, Jr. and Arthur Underwood Jr., *Quantitative Analysis*. New York, Prentice-Hall, 1991.

- 22 J. A. Ratcliffe, *Physics of the Upper Atmosphere*, New York, Academic Press, 1950.
- 23 G. Herzberg, *Molecular Spectra and Molecular Structure*, Vol. II, 2nd ed. New York, Van Nostrand, 1950.
- 24 L.M. Nxumalo and T.A. Ford, *J. Mol. Structure*. 327, 145, 1994.
- 25 M. Bahou et al., *Chem. Phys. Let.*, 265, 145 1997.
- 26 D. Foss Smith and John Overend, *Specrochima Acta* 28A, 87, 1972.
- 27 Schriver-Mazzuoli et al., *J. Chem. Phys.* 102, 690, 1995.
- 28 J. B. Marion and S.T. Thornton, *Classical Dynamics of Particles and Systems*, 4th ed. Philadelphia, Harcourt Brace, 1995.
- 29 H. Kreuger and E. Weitz, *J. Chem. Phys.* 96, 2846, 1992.